Modeling the Thermal Expansion Boundary Layer During the Combustion of Energetic Materials

Igor R. Kuznetsov, D. Scott Stewart*
Eliot Fried
Theoretical and Applied Mechanics, University of Illinois, Urbana, IL 61801, USA

October 27, 2000

Abstract

An approach is presented for modeling the thermal expansion boundary layer in energetic materials such as solid propellants and explosives during their combustion. A thermodynamically consistent system of conservation laws is presented that describes the thermo-elastic solid with a temperature dependent thermal expansion coefficient in order to study the role of thermal expansion in heat transfer and deformation in a thin layer adjacent to the combustion zone. It is shown that the thermal expansion can produce an effect that absorbs energy near the burning surface and can significantly reduce the temperature in a small layer. The analysis given here is also relevant to the technologically important problem of laser ablation of materials, but the the discussion is focused on application to propellant combustion.

Nomenclature:

k	thermal conductivity	μ, λ	elastic coefficients
ρ	density	$\mathbf{E}$	Tensor of deformation
ρ_0	reference density	$\mathbf{F}$	Deformation gradient
m	mass flux	$\mathbf{H}$	Displacement gradient
α	thermal expansion coefficient	ψ	Helmholtz free energy
		$\mathbf{B}$	Left Cauchy-Green tensor
E_y	Young's modulus	ε	internal energy
K	bulk modulus	η	entropy
n	coordinate in the moving frame	ρ	density
		f'	displacement gradient
u	speed of a material particle in the lab. frame	V_f	speed of the regressing (flame) front
ν	Poisson's ratio	T	temperature
σ	stress	T_s	decomposition surface temperature
p_s	Chamber (surface) pressure	T_0	ambient reference temperature
		T_m	melt temperature

*Corresponding author: D. Scott Stewart, Theoretical and Applied Mechanics, University of Illinois, 216 Talbot Laboratory, 104 S. Wright St., Urbana, IL 61081, USA (FAX: 217-244-5707, email: dss@uiuc.edu)

INTRODUCTION

The combustion of energetic materials such as solid propellants and condensed explosives involves extremely complex phenomena. Consider the structure of a nominally steady, regressing solid propellant venting combustion products into a constant pressure atmosphere. Sufficiently deep in the interior of the solid the temperature and stress are uniform, and in the opposite direction, sufficiently far into the gas-region, one encounters gas-phase flames which release energy that maintain the temperature at the surface. As one approaches the combustion surface from within the solid, the temperature in the solid rises due to heat conduction from the hot surface. The solid begins to decompose and suffers thermal expansion and then melts or directly undergoes pyrolysis. Very close to the surface, the formerly solid material may well be a mixture of solid, liquid and gas phases. Many aspects and the relative importance of the physical and chemical processes involved in the decomposition of the solids are still poorly understood. Similar physics is encountered in the study of laser ablation of materials, for example see [1], but the the discussion here is focused on application to propellant combustion.

In a typical solid propellant combustion application, the thermal penetration depth in the solid is very small, on the order of 100 microns or less. The change in temperature across this layer is often on the order of 3000 degrees Kelvin, corresponding to a massive overall temperature gradient in the solid, which in turn can lead to the generation of substantial thermal stresses. At the same time the decomposition processes in this thin layer are critically important in determining the rate of propellant decomposition as well as the material integrity of the solid and its ability to resist degradation by the formation of cracks in the near-surface layer. With advancing technologies that improve both the experimental resolution of the near-surface decomposition layer [2], and simulations that include the complexity of the multi-dimensional, heterogeneous combustion of propellants on the micro-scale, [3], it is very important to carry out studies of known effects such as thermal expansion so as to decide their relative importance. Here we focus on the role of thermal expansion in the solid during combustion and how it affects both the thermal and stress profiles in the near-surface decomposition layer.

In the past some authors have modeled the condensed phase as isothermal, homogeneous and isotropic [4] and used elastic or viscoelastic models to account for the solid deformations. Such models ignore the near-surface thermal layer and should be used only to describe the far-field behaviour of the propellant, well into the interior of the solid. Other approaches treat the solid propellant thermal structure, such as in [5], and solve the energy equation for

the temperature in the solid but neglect the thermal expansion and compressibility effect. Yet another approach solves a heat conduction equation for conducting incompressible solid and after the fact calculates the thermal stresses associated with obtained temperature distribution [6]. Typically the coupling of the thermal stresses with the energy is not taken into account. We do consistently account for this coupling.

Another underlying motivation for our work is to construct simplified models of the propellant combustion interface that are suitable for use in large-scale computer simulation of solid rocket motors, when it is not feasible or desired to resolve the thermal layer. Our analysis must ultimately lead to three-dimensional, tensorially correct jump conditions that are applied at the surface of the solid-propellant. Therefore we use standard methods found in modern continuum mechanics to formulate a thermodynamically consistent, tensorially correct equations that can be used in three-dimensions. The general approach employed here will allow later changes in constitutive theory that can embrace more complex behavior such as viscoelasticity of the solid and more complex phase transitions. We simplify the general formulation to obtain a solution for the temperature and stress field in the solid for a steady, plane regression into a semi-infinite solid that corresponds to the solid half (or portion) of the combined solid-gas propellant flame structure. The thermal profile in the solid is maintained at the surface by the specification of a constant (and elevated) temperature that represents the combustion. Since the formulation is three-dimensional and thermodynamically complete, this solution can be used later to systematically construct more geometrically complex configurations of the near-surface layer, represented as a thin but arbitrarily shaped front, not unlike standard front models used to describe combustion and detonation, [7], [8], [9].

It what follows, the general system of thermomechanical laws of conservation with the entropy inequality are invoked and they are supplemented by an appropriate constitutive theory to determine coupling between the stress and the temperature field. A one-dimensional nonlinear heat equation is derived that describes the temperature solved in the frame of a steady, plane regression into the solid. An exact solution is obtained as well as an asymptotic solution that uses a large parameter introduced to measure the temperature sensitivity of the thermal expansion coefficient near the melt temperature of the solid. Parameter studies of the solutions are carried out to illustrate thermal profiles in two common composite solid propellant constituents that are modeled after AP and HTPB.

FORMULATION

Thermomechanical Laws and Constitutive Theory

The formulation starts with differential form of basic conservation laws in the laboratory frame, $\vec{x}$, for the solid which respectively represents the conservation of mass, linear momentum, angular momentum, energy and the entropy inequality. The dot notation represents the material time derivative.

$$\begin{aligned}
\dot{\rho} &= -\rho\vec{\nabla}\cdot\vec{v}\,, && (1)\\
\rho\dot{\vec{v}} &= \vec{\nabla}\cdot\boldsymbol{\sigma}\,, && (2)\\
\boldsymbol{\sigma} &= \boldsymbol{\sigma}^T\,, && (3)\\
\rho\dot{e} &= -\vec{\nabla}\cdot\vec{q}+\boldsymbol{\sigma}:\vec{\nabla}\vec{v}\,, && (4)\\
\rho\dot{\eta} &\geq -\vec{\nabla}\cdot\left(\frac{\vec{q}}{T}\right)\,. && (5)
\end{aligned}$$

Kinematics

In the thermoelastic solid, both the deformation and the temperature determine the stress and it is necessary to introduce the deformation fields in terms of the definition of the Lagrangian (particle) and Euler (lab-frame) coordinates. Let the coordinates of position in the lab-frame be again given by $\vec{x}$ and the initial position of the particles (or particle coordinates) be given by $\vec{X}$. Then the mapping of the deformations that define the particle trajectory paths is given by

$$\vec{x}=\vec{x}(\vec{X},t)\,. \tag{6}$$

The deformation gradient $\mathbf{F}$ is defined by the tensor

$$\mathbf{F}=\frac{\partial\vec{x}}{\partial\vec{X}}\,, \tag{7}$$

and the velocity of particles $\vec{v}$ is defined by the time derivative of the particle trajectories

$$\vec{v}=\frac{\partial\vec{x}}{\partial t}|_{\vec{X}}\,. \tag{8}$$

The velocity gradient is the divergence of the velocity field and is defined by the tensor

$$\mathbf{L}=\vec{\nabla}\vec{v}\,. \tag{9}$$

A simple and fundamental identity, that can be verified by the previous definitions and the chain rule gives the material (particle-fixed) time derivative of the deformation gradient as

$$\dot{\mathbf{F}} = \mathbf{L}\mathbf{F}\,. \tag{10}$$

Finally from considerations of conservation of mass in the particle frame, one gets a standard result that relates the instantaneous density of the particle ρ to a reference density of not deformed solid at room temperature ρ_0, namely

$$\frac{\rho_0}{\rho} = det(\mathbf{F})\ . \tag{11}$$

Simple Considerations of the Entropy Inequality

Here we briefly review some simple considerations of the entropy inequality that place some restrictions on the form of the constitutive theory for the solid. It is convenient to introduce the Helmholtz free energy ψ which by definition is related to the internal energy, entropy and temperature by

$$e = \psi + T\,\eta\,. \tag{12}$$

We use this relation to solve for the entropy, $\eta = (e-\psi)/T$, take the material derivative and substitute the result into the entropy inequality. One uses the energy equation to replace $\dot{e}$ and simplifies to obtain the intermediate form of the dissipation inequality

$$\boldsymbol{\sigma} : \vec{\nabla}\vec{v} - \rho\dot{\psi} - \rho\eta\dot{T} - \frac{\vec{q}\cdot\vec{\nabla}T}{T} \geq 0\,. \tag{13}$$

A general thermoelastic material can be specified by allowing the Helmholtz free energy to be a function of the deformation gradient and the temperature as $\psi = \psi(\mathbf{F}, T)$, [13]. With this assumption we take the material derivative and use the chain rule and the identity $\dot{\mathbf{F}} = \mathbf{L}\mathbf{F}$ to obtain

$$\dot{\psi} = \frac{\partial\psi}{\partial\mathbf{F}}\mathbf{F}^T : \vec{\nabla}\vec{v} + \frac{\partial\psi}{\partial T}\dot{T}\,. \tag{14}$$

Substitution of the expression for $\dot{\psi}$ into (13) leads to

$$\left(\boldsymbol{\sigma} - \rho\frac{\partial\psi}{\partial\mathbf{F}}\mathbf{F}^T\right) : \vec{\nabla}\vec{v} - \rho\left(\eta + \frac{\partial\psi}{\partial T}\right)\dot{T} - \frac{\vec{q}\cdot\vec{\nabla}T}{T} \geq 0\,. \tag{15}$$

Thus the dissipation inequality (entropy inequality) is satisfied for all physically mechanical and thermal processes (by allowing $\vec{\nabla}\vec{v}$ and $\dot{T}$ range through all admissible valued, independently) if the stress is determined from the potential ψ according to the formula

$$\boldsymbol{\sigma} = \rho \frac{\partial \psi}{\partial \mathbf{F}} \mathbf{F}^T \,, \tag{16}$$

and if the entropy satisfies the Gibbs relation

$$\eta = -\frac{\partial \psi}{\partial T}|_{\mathbf{F}} \,. \tag{17}$$

The remaining term in the reduced dissipation inequality is satisfied if the energy flux vector $\vec{q}$ is determined by the Fourier heat conduction law

$$\vec{q} = -k\vec{\nabla}T \,, \quad \text{with} \quad k \geq 0 \,. \tag{18}$$

Alternate Form of the Energy Equation

In order to determine the coupling between the stress and the temperature field we need to consider an alternative form of the energy equation. Starting with the definition of the Helmholtz free energy, we take the material derivative to obtain

$$\dot{e} = \dot{\psi} + \eta \dot{T} + T\dot{\eta} \,. \tag{19}$$

With the Helmholtz energy of the form $\psi(\mathbf{F}, T)$ and using the Gibbs' relation (17) to replace the derivatives of η with those of ψ we obtain the expression

$$\dot{e} = \frac{\partial \psi}{\partial \mathbf{F}} \mathbf{F}^T : \vec{\nabla}\vec{v} - T\frac{\partial}{\partial T}\left(\frac{\partial \psi}{\partial \mathbf{F}} \mathbf{F}^T : \vec{\nabla}\vec{v}\right) - T\frac{\partial^2 \psi}{\partial T^2}\dot{T} \,. \tag{20}$$

Using the classical definition of the specific heat at constant deformation (volume)

$$C_v \equiv T\frac{\partial \eta}{\partial T}\bigg|_{\mathbf{F}} = -T\left(\frac{\partial^2 \psi}{\partial T^2}\right)\bigg|_{\mathbf{F}} \,, \tag{21}$$

and the previously obtained expression (16) we get the expression

$$\rho\dot{e} = \rho C_v \dot{T} + \boldsymbol{\sigma} : \vec{\nabla}\vec{v} - T\frac{\partial \boldsymbol{\sigma}}{\partial T} : \vec{\nabla}\vec{v} \,. \tag{22}$$

Substitution of this expression back into equation (4) and with the Fourier heat conduction law, we obtain the temperature form for the energy equation

$$\rho C_v \dot{T} = k\nabla^2 T + T\frac{\partial \boldsymbol{\sigma}}{\partial T} : \vec{\nabla}\vec{v}\,. \tag{23}$$

The equation is a heat equation with the appearance of an energy source term that represents the work done by the thermal stresses. If the solid's stress has no temperature dependence then this work term is absent and one obtains the classical heat conduction equation.

Further Specification of the Constitutive Theory

The material described so far is a quite general thermoelastic material with Fourier heat conduction. To apply thermodynamic relation to the particular case of deformation one needs to specify the the form of Helmholtz free energy as a function of the tensor of deformation. We will take ψ to be the sum of three parts, a classical thermal energy density associated with a constant specific heat at a state of zero deformation (constant volume), an elastic potential and a elastic energy density associated with thermal expansion. If we take C_v to be constant and integrate (22) we obtain the thermodynamic potential, ψ_1 for a classical thermally ideal material

$$\psi_1 = C_v(T - T_0) - C_v T log(\frac{T}{T_0})\,, \tag{24}$$

where T_0 is a reference temperature which we take to be solid's ambient temperature.

To describe the elastic potential for isothermal deformation we will use the Blatz-Ko strain energy potential [10]

$$\psi_2 = \frac{\mu}{\rho_0}((I_{\mathbf{B}} - 3) + \frac{1-2\nu}{2\nu}(III_{\mathbf{B}}^{-\frac{\nu}{1-2\nu}} - 1))\,, \tag{25}$$

In the above expression, $\mathbf{B} = \mathbf{F}\mathbf{F}^T$ is the left Cauchy-Green tensor and $I_{\mathbf{B}}$ and $III_{\mathbf{B}}$ are the first and third invariants of $\mathbf{B}$, and are respectively the trace and the determinant of $\mathbf{B}$. Also ρ_0 is the reference density of the solid at room temperature and atmospheric pressure, and the constants μ and ν correspond to Lame constants. In particular this form of the potential allows for the solid to be compressible. In the limit of small strain and Blatz-Ko simply reduces to a standard form of linear elasticity.

An additional elastic potential that accounts for the thermal effects is

$$\psi_3 = -\frac{\alpha K}{2\rho_0}(T - T_0) log(III_{\mathbf{B}})\,, \tag{26}$$

where α is the coefficient of thermal expansion, K is the bulk modulus. Thus our form for the Helmholtz free energy is represented as the sum of the three terms $\psi = \psi_1 + \psi_2 + \psi_3$ or

$$\psi = C_v(T - T_0) - C_v T log(\frac{T}{T_0}) \qquad \text{Thermal energy density}$$

$$+\frac{\mu}{2\rho_0}\left[(I_B - 3) + \frac{1-2\nu}{2\nu}(III_B^{-\frac{\nu}{1-2\nu}} - 1)\right] \qquad \text{Deformation energy density}$$

$$-\frac{\alpha K}{2\rho_0}(T - T_0) log(III_B)\,. \qquad \text{Thermal expansion energy density} \qquad (27)$$

With the chosen form of ψ, we can compute the corresponding forms for the internal energy, entropy and stress tensor in terms of the deformation, $\mathbf{B}$ and the temperature T as

$$e = \psi - T\frac{\partial \psi}{\partial T}\Big|_{\mathbf{B}} = C_v(T - T_0) + \frac{\mu}{\rho_0}((I_{\mathbf{B}} - 3) + \frac{1-2\nu}{2\nu}(III_{\mathbf{B}}^{-\frac{\nu}{1-2\nu}} - 1)) + \frac{\alpha K}{2\rho_0} T_0 log(III_{\mathbf{B}})\,, \quad (28)$$

$$\eta = -\frac{\partial \psi}{\partial T}\Big|_{\mathbf{B}} = C_v log(\frac{T}{T_0}) + \frac{\alpha K}{2\rho_0} log(III_{\mathbf{B}})\,, \quad (29)$$

$$\boldsymbol{\sigma} = 2\rho\frac{\partial \psi}{\partial \mathbf{B}}\boldsymbol{B} = \mu\frac{\rho}{\rho_0}(\mathbf{B} - III_{\mathbf{B}}^{-\frac{\nu}{1-2\nu}}\mathbf{I}) - \alpha K\frac{\rho}{\rho_0}(T - T_0)\mathbf{I}\,. \quad (30)$$

(Note that in computing the stress from the deformation energy the following relations are useful, namely $\partial(I_{\mathbf{B}})/\partial\mathbf{B} = \boldsymbol{I}$ and $\partial(III_{\mathbf{B}})/\partial\mathbf{B} = III_{\mathbf{B}}\mathbf{B}^{-1}$.)

Small Strain and Contributions Due to Thermal Stress

The small strain assumption is represented by writing

$$\mathbf{F} = \mathbf{I} + \mathbf{H}\,, \quad (31)$$

where $\mathbf{I}$ is the identity tensor and $\mathbf{H}$ is the displacement gradient tensor, and the the tensor normal of $\mathbf{H}$ is small. The left Cauchy-Green tensor $\mathbf{B}$ is written in terms of $\mathbf{H}$ as

$$\mathbf{B} = \mathbf{F}\mathbf{F}^T = \mathbf{I} + \mathbf{H} + \mathbf{H}^T + \mathbf{H}\mathbf{H}^T = \mathbf{I} + 2\mathbf{E} + \mathbf{H}\mathbf{H}^T\,, \quad (32)$$

and its linearization is simply $\mathbf{B} = 1 + 2\mathbf{E}$, where $\mathbf{E} = (\mathbf{H} + \mathbf{H}^T)/2$ is the small deformation strain tensor. From that it follows that the determinant of $\mathbf{F}$ is approximated by

$$\frac{\rho}{\rho_0} = III_{\mathbf{B}}^{-1/2} = (1 + 2I_{\mathbf{E}})^{-1/2} \quad (33)$$

and we obtain a classical formula for the thermoelastic stress tensor

$$\boldsymbol{\sigma} = 2\mu\,\mathbf{E} + \lambda I_{\mathbf{E}}\mathbf{I} - \alpha K(T - T_0)\,\mathbf{I}\,, \tag{34}$$

where $\lambda = 2\mu\,\nu/(1-2\nu)$ and where $I_{\mathbf{E}}$ is the tr$\mathbf{E}$.

Data on the temperature dependence of the thermal expansion coefficient and density for the constituents of energetic materials such as AP, HMX and binder materials is often scarce and sometimes not available in the literature. A study by Zanotti et al [11] presents experimental data for k, C_v , and suggests that within temperature range of normal combustion regimes for AP those properties wary, but not very much. The temperature dependence appear to be linear and weak. At the same time, experimental data for plastics, other binder materials and organic salts similar to AP, found in [12], shows much stronger temperature dependence for thermal expansion coefficient near the transition temperature (which maybe the melt temperature or a sublimation temperature). Not only does the coefficient of thermal expansion change significantly with increasing temperature, but the temperature derivative of the coefficient of thermal expansion can take large values near melting point.

Since the thermal stress-work term in the energy equation is proportional to $\partial\boldsymbol{\sigma}/\partial T$ and if we differentiate (34) with respect to T we find that

$$\frac{\partial\boldsymbol{\sigma}}{\partial T} = -K\left(\alpha + \frac{\partial\alpha}{\partial T}(T - T_0)\right)\mathbf{I}\,, \tag{35}$$

so a material with thermal expansion coefficient with a moderate value, but with a large derivative near a melt or transition temperature can possibly generate significant work due to the thermal stresses. These considerations have led us to retain the temperature dependence on the coefficient of thermal expansion coefficient.

STEADY PLANAR REGRESSION

We specialize our considerations to one-dimensional deformations and regression of the solid. For one-dimensional deformations the mapping between the Euler and Lagrangian coordinates is specified

$$x_1 = x_1(X_1, t) = X_1 + f(X_1, t)\,, \quad x_2 = X_2\,, \quad x_3 = X_3\,, \tag{36}$$

and $\partial/\partial x_2 = \partial/\partial x_3 = 0$. There is one non-zero velocity component that we denote by $u_1 = u$. Also let $x_1 = x$ to simplify the presentation. The corresponding components of

the deformation gradient $\mathbf{F} = \partial\vec{x}/\partial\vec{X}$, Left-Cauchy Green tensor, $\mathbf{B} = \mathbf{F}\mathbf{F}^T$, small strain tensor $\mathbf{E} = (\mathbf{H} + \mathbf{H}^T)/2$ are computed as

$$\mathbf{F} = \begin{bmatrix} 1+f' & 0 & 0 \\ 0 & 1 & 0 \\ 0 & 0 & 1 \end{bmatrix}, \quad \mathbf{B} = \mathbf{F}\mathbf{F}^T = \begin{bmatrix} (1+f')^2 & 0 & 0 \\ 0 & 1 & 0 \\ 0 & 0 & 1 \end{bmatrix}, \quad \mathbf{E} = \begin{bmatrix} f' & 0 & 0 \\ 0 & 0 & 0 \\ 0 & 0 & 0 \end{bmatrix}, \tag{37}$$

The velocity gradient becomes

$$\mathbf{L} = \vec{\nabla}\vec{v} = \begin{bmatrix} \frac{\partial u}{\partial x} & 0 & 0 \\ 0 & 0 & 0 \\ 0 & 0 & 0 \end{bmatrix}. \tag{38}$$

The stress tensor has one non-zero component

$$\sigma \equiv \sigma_{11} = (2\mu + \lambda)f' - \alpha K(T - T_0)\,. \tag{39}$$

Next we introduce the traveling wave coordinate for an observer traveling at the regression speed of the decomposition interface (i.e the regression speed associated with the combusiton of the solid propellant),

$$n = x - V_f t\,, \tag{40}$$

such that the decomposition interface is located at $n = 0$, and the domain of solid propellant is unbounded on the right. The decomposition surface is advancing to the right at a constant velocity $V_f > 0$. It follows that

$$\frac{\partial}{\partial x} = \frac{\partial}{\partial n}\,, \quad \frac{\partial}{\partial t}|_{\vec{x}} = -V_f \frac{\partial}{\partial n}\,. \tag{41}$$

Later we will need the relation between the deformation gradient and the velocity gradient. The general kinematic identity $\dot{\mathbf{F}} = \mathbf{L}\mathbf{F}$ when specialized to one-dimensional deformations in the steady moving frame becomes

$$(u - V_f)\frac{df'}{dn} = \frac{\partial u}{\partial n}(1 + f')\,. \tag{42}$$

We also note that the mass conservation statement (11) that relates the density to the reference density now simply reduces to

$$\rho = \frac{\rho_0}{1 + f'}\,. \tag{43}$$

Boundary Conditions

The temperature is assumed to be the ambient temperature far into the interior $T(\infty) = T_0$ and at the decomposition surface we assume the temperature be a constant $T(0) = T_s$, where $T_s > T_0$. The stress is maintained by the pressure in the combustion chamber with the value at the surface $p(0) = p_s$. The applied stress at the surface causes induces deformation and far enough into the interior of the solid the strain is constant. We assume that there is a confining wall that supports the solid against the pressure imposed by the chamber. Hence in the far-field, $u(\infty) = 0$.

Structure Equations for the Thermal Layer in the Solid

With the previous assumptions the governing equations reduce to a system of ordinary differential equations in the steady regression coordinate n. It is a simple matter to integrate the mass and momentum energy equation across the structure and evaluate the constants of integration in the interior of the solid. The once integrated mass, linear-momentum equations becomes

$$\rho(u - V_f) = -\rho_\infty V_f = m\,, \tag{44}$$

$$mu = \sigma + p_\infty\,. \tag{45}$$

The energy equation becomes

$$C_v m\frac{dT}{dn} = k\frac{d^2T}{dn^2} + T\frac{\partial\sigma}{\partial T}\frac{\partial u}{\partial n}\,. \tag{46}$$

The derivative of the stress with respect to temperature is $\partial\sigma/\partial T = -K(\alpha + d\alpha/dT(T - T_0))$ so that the revised energy equation becomes

$$C_v m\frac{dT}{dn} = k\frac{d^2T}{dn^2} - KT\left[\alpha + \frac{\partial\alpha}{\partial T}(T - T_0)\right]\frac{\partial u}{\partial n}\,. \tag{47}$$

We turn to deriving an expression to replace the velocity gradient $\partial u/\partial n$ in term of the temperature, next.

¿From mass conservation in the steady regressing frame we solve for the particle velocity as $u = m/\rho + V_f$, and with $\rho = \rho_0/(1 + f')$, we obtain the intermediate result for the regression velocity $V_f = -m/\rho_\infty = -m(1 + f'_\infty)/\rho_0$, where the result has been evaluated far in the interior of the solid. (Note that if $V_f > 0$ then $m < 0$.) Replacing V_f in the previous

expression obtains the the particle velocity in terms of the mass flux and displacement gradient

$$u = \frac{m}{\rho_0}(f' - f'_\infty)\,. \tag{48}$$

Next we substitute these result into the once integrated form for the momentum equation (45), use the expression for the stress and then solve for the deformation gradient f' in terms of the temperature to obtain

$$f' = \frac{-\alpha K(T - T_0) + p_\infty + (m^2/\rho_0)f'_\infty}{m^2/\rho_0 - (2\mu + \lambda)}$$

Also the pressure in the interior is simply related to the deformation gradient there by the simple formula (evaluated from the expression for the stress) as $p_\infty = -(2\mu + \lambda)f'_\infty$. (It also follows that $\rho_\infty = \rho_0/[1 - p_\infty/(2\mu + \lambda)]$.) So we can use this to rearrange the previous formula to obtain a simpler one

$$f' = f'_\infty - \frac{\alpha K(T - T_0)}{m^2/\rho_0 - (2\mu + \lambda)} \tag{49}$$

Now differentiate this expression with respect to the regression coordinate n to obtain

$$\frac{df'}{dn} = -\frac{K}{m^2/\rho_0 - (2\mu + \lambda)}\left[\alpha + (T - T_0)\frac{d\alpha}{dT}\right]\frac{dT}{dn}\,. \tag{50}$$

Since $\partial u/\partial n = (m/\rho_0)df'/dn$, we can rewrite the stress-work source term in the energy equation as a function of the temperature and obtain the nonlinear heat equation

$$\frac{dT}{dn} = \left(\frac{k}{mC_v}\right)\frac{d^2T}{dn^2} + \frac{K^2}{C_v[m^2 - \rho_0(2\mu + \lambda)]}\left[\alpha + (T - T_0)\frac{d\alpha}{dT}\right]^2 T\frac{dT}{dn}\,. \tag{51}$$

which is to be solved subject to the boundary conditions that $T(0) = T_s$ and $T(\infty) = T_0$. It is clear that in the absence of thermal expansion this equation reduces to the classical heat equation and the solution is the classical exponential profile.

Once the temperature profile is determined, then the displacement gradient f' can be evaluated from formula (49) and the stress is directly evaluated from the stress formula, expressed below as

$$\sigma = -p_\infty - \alpha K(T - T_0)\left(1 + \frac{(2\mu + \lambda)}{m^2/\rho_0 - (2\mu + \lambda)}\right)\,. \tag{52}$$

The stress in the propellant consists of a constant due to simple elastic deformation plus a contribution due to thermal expansion.

Equation (51) is an autonomous second order ODE that can be solved analytically, and before we do that we'll write it in nondimensional form. To avoid the introduction of new symbols, from this point on, we will use a tilde to designate a dimensional quantity and the absence of tilde - a dimensionless one. Let $\tilde{n} = |\tilde{k}/(\tilde{m}\tilde{C}_v)|\, n$, with the characteristic length of the thermal boundary layer thickness for incompressible solid, $|\tilde{k}/(\tilde{m}\tilde{C}_v)|$. We take the surface temperature $\tilde{T}_s$ to be the characteristic temperature so that $\tilde{T} = \tilde{T}_s\, T$. (This choice sets the dimensionless surface temperature to be unity.) Finally we choose a temperature sensitive functional form for $\alpha(T)$ that reflects a rapid (exponential) change as the temperature nears the melt temperature. We suppose that

$$\tilde{\alpha} = \tilde{\alpha}_\infty \left[1 + \tilde{b} \exp(-\tilde{\theta}(1/\tilde{T} - 1/\tilde{T_m}))\right] , \tag{53}$$

where $\tilde{\alpha}_\infty$ is the thermal expansion coefficient in the cold solid and the dimensional constant $\tilde{\theta}$ (with units of temperature) measures the rate of change of $\tilde{\alpha}$ near the melt temperature. The constant $\tilde{b}$ measures the magnitude of the change from the base value, $\tilde{\alpha}_\infty$.

Our search of the literature has yeilded only base values for the thermal expansion coefficients for AP and HTPB, which are shown in Table 1. However thermal expansion data is available for more common materials, which includes plastics like PMMA, for example. Fig 1. shows that PPMA exhibits a nearly 7-fold increase in the thermal expansion coefficient over a temperature range of 250 degrees Kelvin and a substantial change in the derivative of the same with respect to temperature near the melting point. Similarily organic salts like AP show large, dramatic changes in the thermal expansion coefficient near the transition temperatures. In lieu of better information regarding $\tilde{\alpha}(\tilde{T})$ equation (53) can be regarded as a model of the same dependence with two adjustable parameters, and hence we study the dependence of the effect of the thermal expansion layer in terms of them. For example, Fig. 2. shows a plot of $\tilde{\alpha}(\tilde{T})$ as for values that correspond to AP.

For the purposes of the subsequent asymptotic description it is convenient to redefine the constant $b = \tilde{b} \exp(-\theta(1 - T_s/T_m))$, so that

$$\tilde{\alpha} = \tilde{\alpha}_\infty \left[1 + b \exp(-\theta(1/T - 1))\right] , \tag{54}$$

where $\theta = \tilde{\theta}/\tilde{T}_s$. Then equation (51) is re-written as

$$-\frac{dT}{dn} = \frac{d^2T}{dn^2} - \left(\frac{\tilde{\alpha}_\infty^2 \tilde{K}^2 \tilde{T}_s}{\tilde{C}_v(\tilde{m}^2 - \tilde{\rho}_0(2\tilde{\mu} + \tilde{\lambda})}\right) \left[1 + be^{-\theta(1/T-1)} \left(1 + \frac{\theta(T - T_0)}{T^2}\right)\right]^2 T\frac{dT}{dn} \tag{55}$$

to be solved subject to the boundary conditions $T(0) = 1$ and where $T(\infty) = T_0$, with $T_0 = \tilde{T}_0/\tilde{T}_s$.

Table 1. Parameter Values Used to Describe AP and HTPB

$\tilde{k}_{AP}$	=	$0.58(W/mK)$	$\tilde{k}_{HTPB}$	=	$0.21(W/mK)$
$\tilde{C}_{p\,AP}$	=	$1.54 \times 10^3(J/kgK)$	$\tilde{C}_{p\,HTPB}$	=	$2.83 \times 10^3(J/kgK)$
$\tilde{\rho}_{0\,AP}$	=	$1880(kg/m^3)$	$\tilde{\rho}_{0\,HTPB}$	=	$880(kg/m^3)$
$\tilde{m}$	=	$-17(kg/m^2sec)$	$\tilde{\mu}$	=	$1.2 \times 10^6(Pa)$
$\tilde{\alpha}_\infty$	=	$1.4 \times 10^{-4}(1/K)$	$\tilde{\lambda}$	=	$59 \times 10^7(Pa)$
$\tilde{E}_y$	=	$3,585(kPa)$	$\tilde{\nu}$	=	0.499
$\tilde{K}$	=	$6 \times 10^8(Pa)$	$\tilde{C}_p/\tilde{C}_v$	=	1.22
$\tilde{p}_s$	=	$10^6(Pa)$			

Results

Equation (55) is solved directly by two succesive integrations and its solution is represented by an implicit function $T(n)$ as

$$\int_1^T \frac{dT}{\int_{T_0}^T (1 - \mathcal{F}(t,\theta)t)dt} = n\,, \tag{56}$$

where

$$\mathcal{F}(T,\theta) = \left(\frac{\tilde{\alpha}_\infty^2 \tilde{K}^2 \tilde{T}_s}{\tilde{C}_v(\tilde{m}^2 - \tilde{\rho}_0(2\tilde{\mu} + \tilde{\lambda}))}\right)\left[1 + be^{-\theta(1/T-1)}\left(1 + \frac{\theta(T - T_0)}{T^2}\right)\right]^2 .$$

Indeed for given parameters, the above formula can be evaluated to plot the temperature profile in the solid. (Note, we could have choosen an entirely different functional form for $\alpha(T)$ and derived a similar result.) In the following sections we will evalute this exact solution which in turn does exhibit a thermal expansion boundary layer near the decomposition surface. But in order to make the nature of the result clear, we develop an asymptotic analysis of the boundary layer in the limit of large θ, and describe this analysis next.

Asymptotic Solution

We will consider surface temperature close to or at the melt temperature in order to ensure that our material might be described as an elastic solid. Assume the ratio of the surface temperature to the melt temperature is

$$\tilde{T}_s/\tilde{T}_m = 1 - \delta/\theta\,, \tag{57}$$

where δ is an $O(1)$ constant. Our temperature equation is rewritten as

$$-\frac{dT}{dn} = \frac{d^2T}{dn^2} + A(1-\delta/\theta)\left[1 + b\, e^{-\theta(\frac{1}{T}-1)}\left(1 + \frac{\theta(T-T_0)}{T^2}\right)\right]^2 T\frac{dT}{dn}\,, \tag{58}$$

where the parameter A is defined by

$$A = \left|\frac{\tilde{\alpha}_\infty^2 \tilde{K}^2 \tilde{T}_m}{\tilde{C}_v(\tilde{m}^2 - \tilde{\rho}_0(2\tilde{\mu}+\tilde{\lambda}))}\right|\,. \tag{59}$$

The parameter A can be estimated for typical solid propellant applications for various constitutents. For example, for a regression velocity of approximately $V_f = 1\, cm/sec$, using the values in Table 1. for AP, we find that A is approximately 10^{-3}. We use that fact shortly.

Simple consideration of equation (58) suggests that there are two layers. The outer layer lies in the interior of the solid where $T < 1$, well below the surface temperature. The temperature dependence of the thermal expansion coefficient is exponentially weak and if A is sufficiently small, one obtains the standard exponential profile corresponding to the heat equation without the thermal expansion losses. However near the hot surface the effect thermal expansion can play a role. Based on the assumption of a near-surface boundary layer we introduce the layer coordinate coordinate $s = n\,\theta$ and look for the inner solution in the form

$$T_{inner}(s) = 1 + \frac{1}{\theta}t^{(1)}(s) + \dots\,. \tag{60}$$

In this layer, diffusion is always a dominant effect and advection is uniformly small. A balance of terms with the largest contribution from the thermal expansion leads to the equation

$$\frac{d^2t^{(1)}}{ds^2} = -qe^{2t^{(1)}}\frac{dt^{(1)}}{ds} \quad \text{with} \quad q = Ab^2\theta(1-T_0)^2\,, \tag{61}$$

and requires us to consider a distinguished limit where $Ab^2\theta \sim O(1)$. Since A is physically estimated to be a value of $O(10^{-3})$ and we anticipate an order of magnitude thermal coefficient expansion coefficient near the melt temperature (a factor of 5 or 6 is typical in plastics and salts, for example), we suppose that b could large, and we choose to study the formal asymptotic limit

$$A = \hat{A}\frac{1}{\theta^3}, \quad b = \hat{b}\theta, \quad \text{with} \quad \hat{A} = O(1),\, \hat{b} = O(1)\,, \quad \text{as} \quad \theta \to \infty\,. \tag{62}$$

The solution to (61) is

$$t^{(1)}(s) = \frac{1}{2}\ln\left(\frac{-c_1}{e^{[2\,c_1(c_2-s)]} - q/2}\right), \qquad c_1 < 0\,, \tag{63}$$

and applying the boundary condition at the origin, $t^{(1)}(0) = 0$, we determine the relation between the constants $c_2 = \frac{1}{2}\ln(q/2 - c_1)$ and write the two-term inner solution in terms of c_1 as

$$T_{inner} = 1 + \frac{1}{2\theta}\ln\frac{-c_1}{(\frac{1}{2}q - c_1)e^{-2c_1 s} - q/2}\,. \tag{64}$$

The remaining constant c_1 will be obtained from matching with the outer solution.

If we assume an expansion for the outer solution in the form

$$T_{outer} = T^{(0)}(n) + \frac{1}{\theta}T^{(1)}(n) + \dots\,, \tag{65}$$

substitution into (58) obtains

$$\frac{dT^{(0)}}{dn} = -\frac{d^2T^{(0)}}{dn^2}, \qquad T^{(0)}(0) = 1, \qquad T^{(0)}(\infty) = T_0\,, \tag{66}$$

$$\frac{dT^{(1)}}{dn} = -\frac{d^2T^{(1)}}{dn^2}, \qquad T^{(1)}(\infty) = 0\,, \tag{67}$$

which generates to the two term outer-solution

$$T_{outer}(n) = (1 - T_0)e^{-n} + T_0 + \frac{1}{\theta}C_3 e^{-n} + \dots\,. \tag{68}$$

Matching of the inner and outer expansion determines the constants

$$c_1 = (T_0 - 1), \qquad C_3 = \frac{1}{2}\ln(\frac{T_0 - 1}{T_0 - 1 - q/2})\,. \tag{69}$$

Finally based on these determinations, the two-term composite expansion is

$$\begin{aligned} T(n) \;&= (1 - T_0)e^{-n} + T_0 + \frac{1}{2\theta}e^{-n}\ln\left[\frac{T_0 - 1}{T_0 - 1 - q/2}\right] \quad \text{Outer} \\ +\;&\quad 1 + \frac{1}{2\theta}\ln\left[\frac{1 - T_0}{(q/2 - T_0 + 1)e^{2(1-T_0)n\theta} - q/2}\right] \quad \text{Inner} \\ -\;&\quad \left(1 + (T_0 - 1)n + \frac{1}{2\theta}\ln\left[\frac{T_0 - 1}{T_0 - 1 - q/2}\right]\right) \quad \text{Common part} \end{aligned} \tag{70}$$

With this explicit dependence formula for $T(n)$ we can calculate the dimensionless heat flux at the surface as

$$\frac{dT}{dn}(0) = -(1-T_0) - \frac{1}{2}q - \frac{1}{2\,\theta}\ln\frac{T_0-1}{T_0-1-q/2} + \dots \,. \tag{71}$$

The first term on the RHS stands for the heat flux calculated without taking thermal expansion into account, and the latter terms are the corrections due to thermal expansion.

Parametric Studies

Here we discuss the properties of the solutions for the temperature and stress distributions in the regression wave, and for purposes of illustration we use AP and HTPB properties. We take the rough estimate of the melt temperature for AP to be T_m=700 K and for HTPB to be 450 K. Again note that parameter b measures the change in α/α_∞ over the temperature range between T_0 and T_m. Figure 2 shows $\alpha(T)$ for two sets values of b, θ, for values that otherwise correspond to AP.

Figure 3 shows typical dimensionless temperature profiles in the solid for A = 0.0035 (which corresponds to AP); b = 30, 50; θ=10. The dashed line is for $\alpha = \alpha_\infty = constant$ and the solid line is the evaluation of the exact solution to (56). The constant b is chosen to be large in order to illuminate the difference between the two cases shown. The sharp decrease in temperature in the boundary layer is accounted for by the thermal expansion work term in the energy equation and consequently there is an additional heat drawn into the solid due to the expansion near the surface.

Figures 4, 5 display the dimensional profiles for AP, HTPB for A=0.0035 and A=0.0026 respectively, and for the same set of values of b, θ as in Fig 3. With the same melt temperatures and with $\delta = 0$ ($T_s = T_m$), the penetration depth and thermal boundary layer thickness is quite different for AP and HTPB mainly due to the differences in their thermal conductivities.

Deformation gradients for AP, HTPB are presented on Fig.6. The significant changes in the gradient are due to expansion and are confined to approximately 10μ for AP and 1μ for the HTPB. We see that, while remaining negative far enough from the surface, the deformation gradient becomes positive in the boundary layer. The material, not confined at the surface, swells and expands outwards, locally decreasing the absolute value of the displacement in that region. One can expect that the essential difference in the length scale of this effect for propellant constituents generate gaps and tears in the composite energetic material and may result in mechanical separation of AP grains from the binder, but those effects can not be studied in this current one dimensional framework. Figure 7 shows the displacement, both nondimensional and for AP, for the finite layer of burning material.

Displacement is a linear function of coordinate far enough in the solid, where material is compressed, while in the boundary layer the thermal expansion effect takes over and reduces compression or even makes the material swell.

As we already mentioned, the model assumes that the temperature of the surface T_s, which is in general less or equal to T_m. To illustrate how the endothermic effect in the near-surface layer depends on the difference between T_s and T_m, we take three values of $\delta = 0, 1.5, 2.5$ and plot three pairs of curves for α=const and for θ=10, b=30, shown in Fig. 7. We see that the greatest difference is observed for δ=0, and with the increase of δ it becomes less pronounced.

Figure 8. show the value of the dimensionless surface temperature gradient as a function of b for a fixed value of θ. Figure 10 shows a contours of the increase in the dimensional heat flux to the surface (computed with AP values) as a function of parameters b, θ with $\delta = 0$ ($T_m = T_s$) relative to a base case where $b = 0$, $\alpha = \alpha_\infty = constant$. Note that the heat flux to the solid is increased significantly from that of the base case even for modest values of the parameters b and θ. For example, one can pick $b = 10$ and $\theta = 10$ and get a 100 percent increase in the heat flux to the solid given a fixed surface temperature.

In a study that considered the temperature dependent thermal conductivity in the solid, Bloomshield and Osborn [14] showed that the temperature in the solid can be lowered from the classical profile that is computed with constant material properties. Cited experimentally obtained profiles also showed lower temperatures than those calculated with constant mateial properties. Here we have shown that changes in the temperature profiles can be affected by work losses due to temperature dependent thermal expansion. Future studies that include both effects are warranted.

CONCLUSIONS

A simple but thermodynamically consistent model of thermal boundary layer in solid phase of energetic material during combustion has been developed to account for the thermal expansion. It was shown that temperature dependent thermal expansion results in a formation of a thin region near the surface where energy is consumed by thermal expansion work, leading to decrease in temperature and sharpening of the temperature gradient at the surface. Enhancement of the heat flux into the surface is obtained due to the lower of the temperature profile in the solid due to energy deposited in the solid due to the expansion. In addition, if the thermal expansion is temperature dependent there are significant deformation gradients (strains) near the surface in a small boundary layer. Two constituents of

solid propellants were studied as representative, AP and HTPB and some essential differences, mainly based on the difference in penetration depth and boundary layer thickness was observed.

Our discussion should be viewed as a qualitative one since there are uncertainties in the material properties for particular constituents and precise quantitative evaluation is not easily done. Nevertheless, these results provide an insight into the physics of the phenomena and can be used in future modeling efforts.

ACKNOWLEDGEMENTS

The University of Illinois Center for Simulation of Advanced Rockets research program is supported by the US Department of Energy through the University of California under sub contract B341494. D. S. Stewart has also been supported by Los Alamos National Laboratory, DOE/LANL I2933-0019

References

[1] Duley, W. W., *UV Lasers: Effects and Applications in Materials Science*, Cambridge University Press, (1996).

[2] Hanson-Parr, D.M., Parr, T.P., Thermal Properties Measurements of Solid Rocket Propellant Oxidizers and Binder materials as a Function of Temperature. China-Lake, CA, 1997.

[3] Hegab, A., Jackson, T. L., Buckmaster, J. and Stewart, D. S., Nonsteady Burning of Periodic Sandwich Propellants with Complete Coupling Between the Solid and Gas Phases, preprint (2000), submitted to *Combustion and Flame*.

[4] Kuo, K.K., Kooker, D.E., Coupling Between Nonsteady Burning and Structural Mechanics of Solid-Propellant Grains ,in Progress in Astronautics and Aeronautics, Vol. 143, AIAA Inc., 1992.

[5] Ward, M.J., Son, S.F., Brewster, M.Q., Steady Deflagration of HMX with Simple Kinetic. Combustion and Flame J., vol 114, 1998.

[6] Landau, L.D., Lifshiz, E.M., Theory of Elasticity. Pergamon Press, London, 1959.

[7] Pelce, P., Clavin, P., Influence of hydrodynamics and diffusion upon the stability limits of laminar premixed flames. J. Fluid Mech., Vol 124, page 219 (1982)

[8] Matalon, M., Matkowsky, B. J., Flames as gasdynamic discontinuities (1982) J. Fluid Mech., Vol. 124, Page 239 (1982)

[9] Stewart, D. S. The shock dynamics of multi-dimensional condensed and gas phase detonations. Proceedings of the 27th International Symposium on Combustion, pp. 2189-2205 (1998)

[10] Drozdov, A.D., Finite Elasticity and viscoelasticity. World Scientific, 1996.

[11] Zanotti, C., Volpi, A., Measuring Thermodynamic Properties of Burning Propellant , in Progress in Astronautics and Aeronautics, Vol. 143, AIAA Inc., 1992.

[12] Thermodynamical Properties of Matter. TPAC Data Series, Vol. 13, Plenum Publishing, New York, NY, 1997 pp. 1470-1473.

[13] Bowen, R.M., Introduction to Continuum Mechanics for Engineers. Plenum Press, New York, NY, 1989.

[14] Bloomshield, F.S., Osborn, J.R., Effect of Variable solid phase properties on propellant combustion, Acta Astronautica, Vol.12, No.12, pp. 1017-1025, (1985).

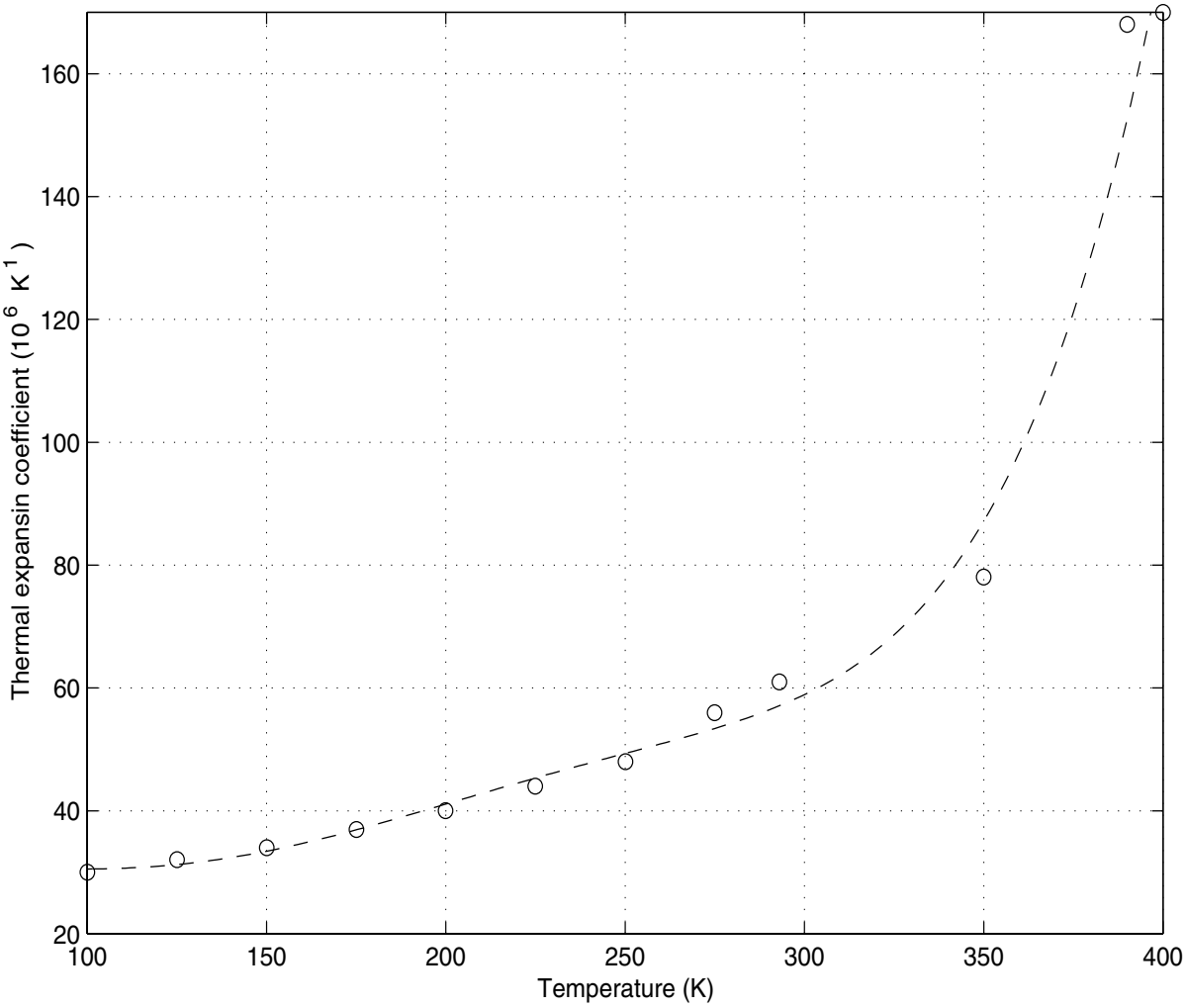

Figure 1: Experimental data for PMMA thermal expansion coefficient [7].

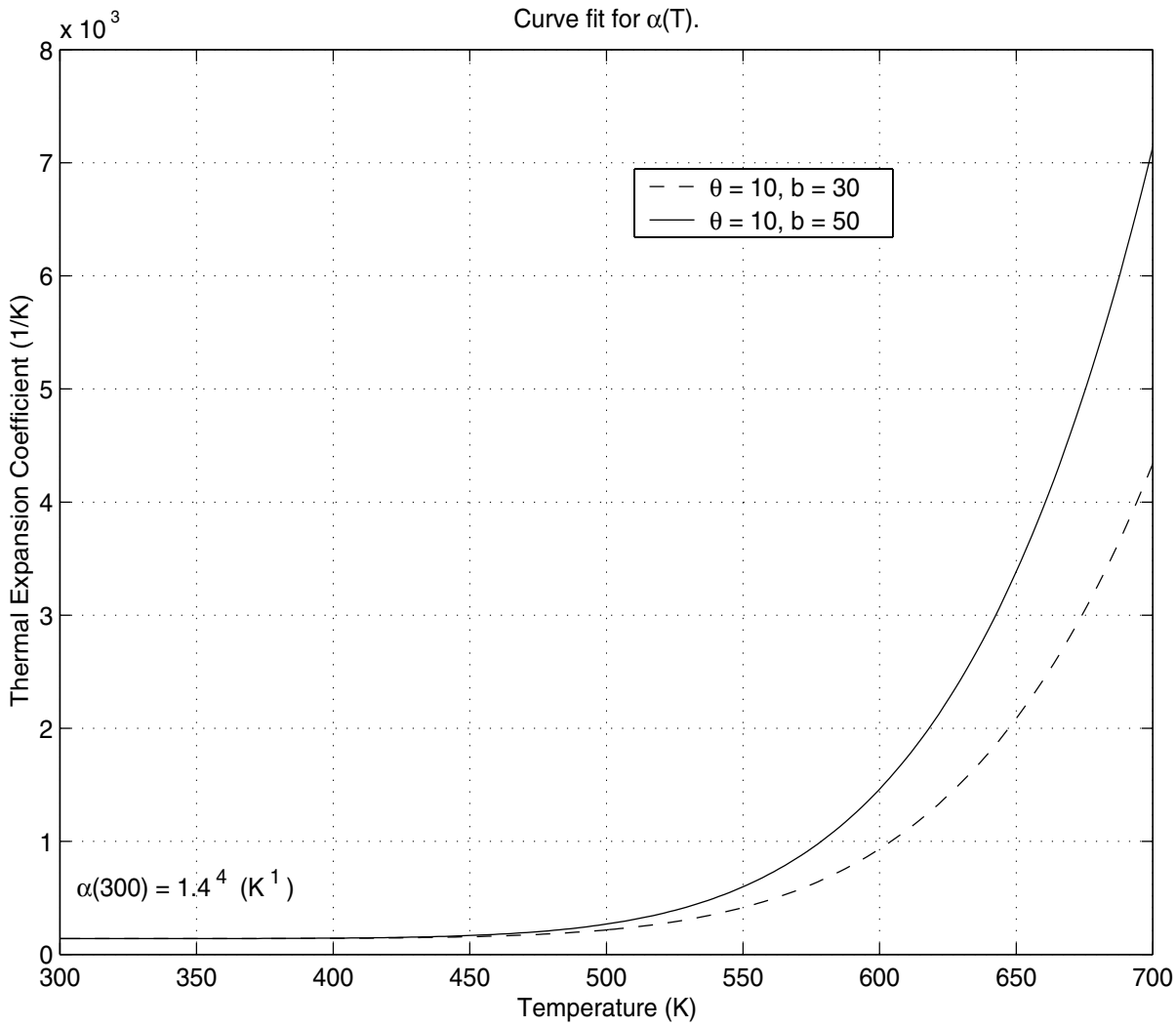

Figure 2: Curve fit for the thermal expansion coefficient as a function of temperature for AP.

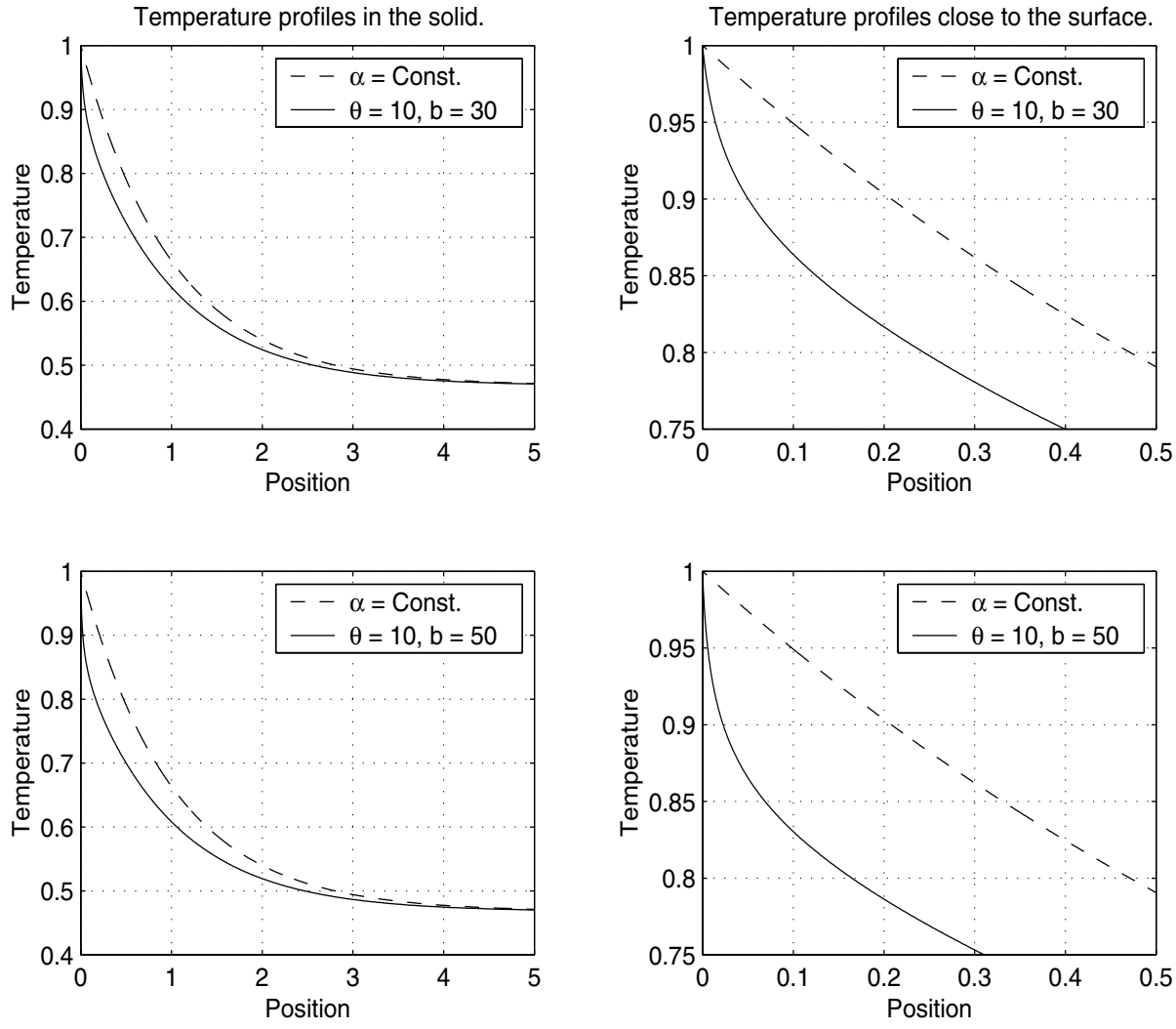

Figure 3: Nondimensional temperature profiles T(n) for two sets of curve fit parameters θ and b for $\alpha(T)$. Dotted line represents material with constant thermal expansion coefficient α_∞.

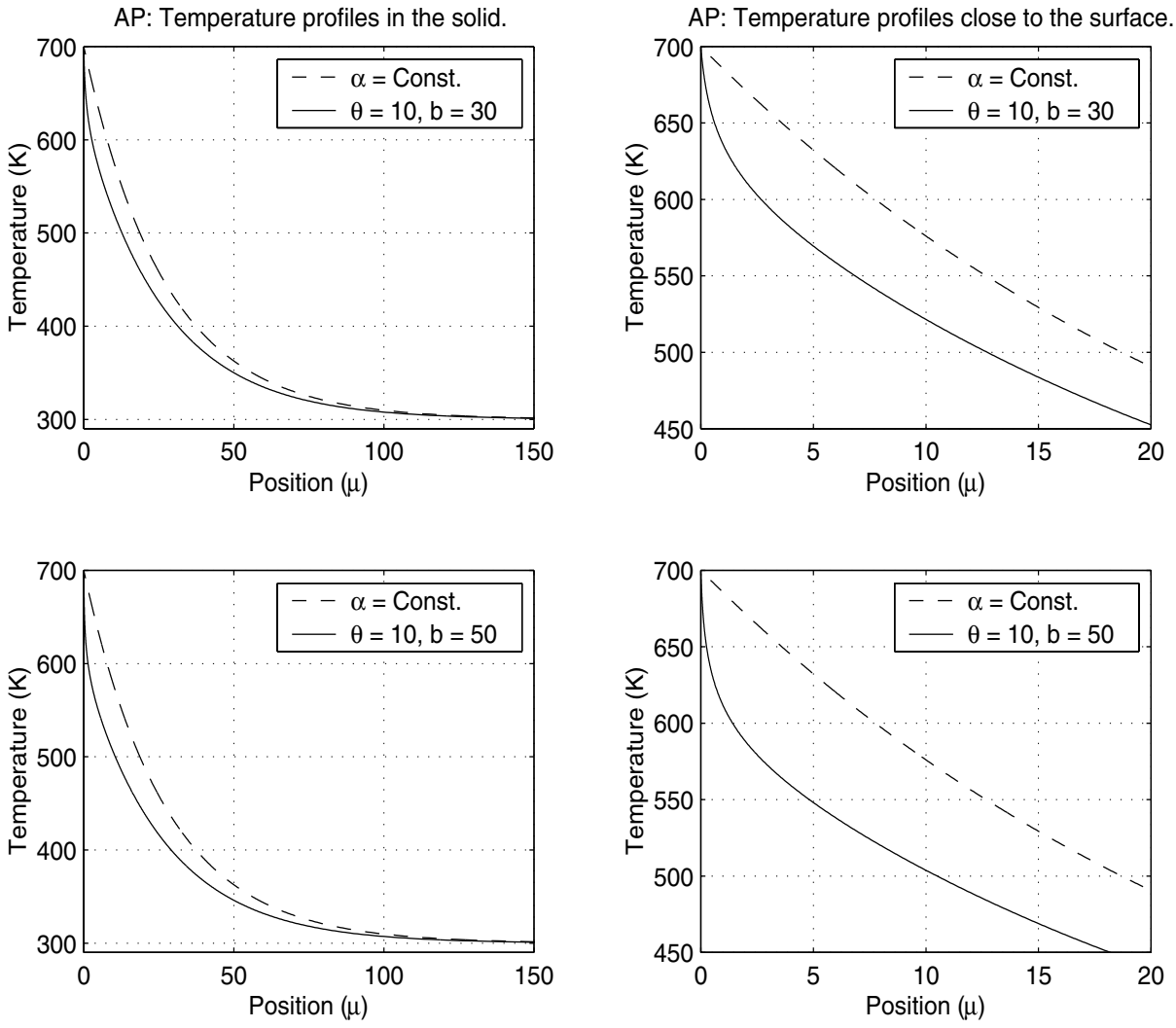

Figure 4: AP temperature profiles T(n) for two sets of curve fit parameters θ and b for $\alpha(T)$. Dotted line represents material with constant thermal expansion coefficient α_∞.

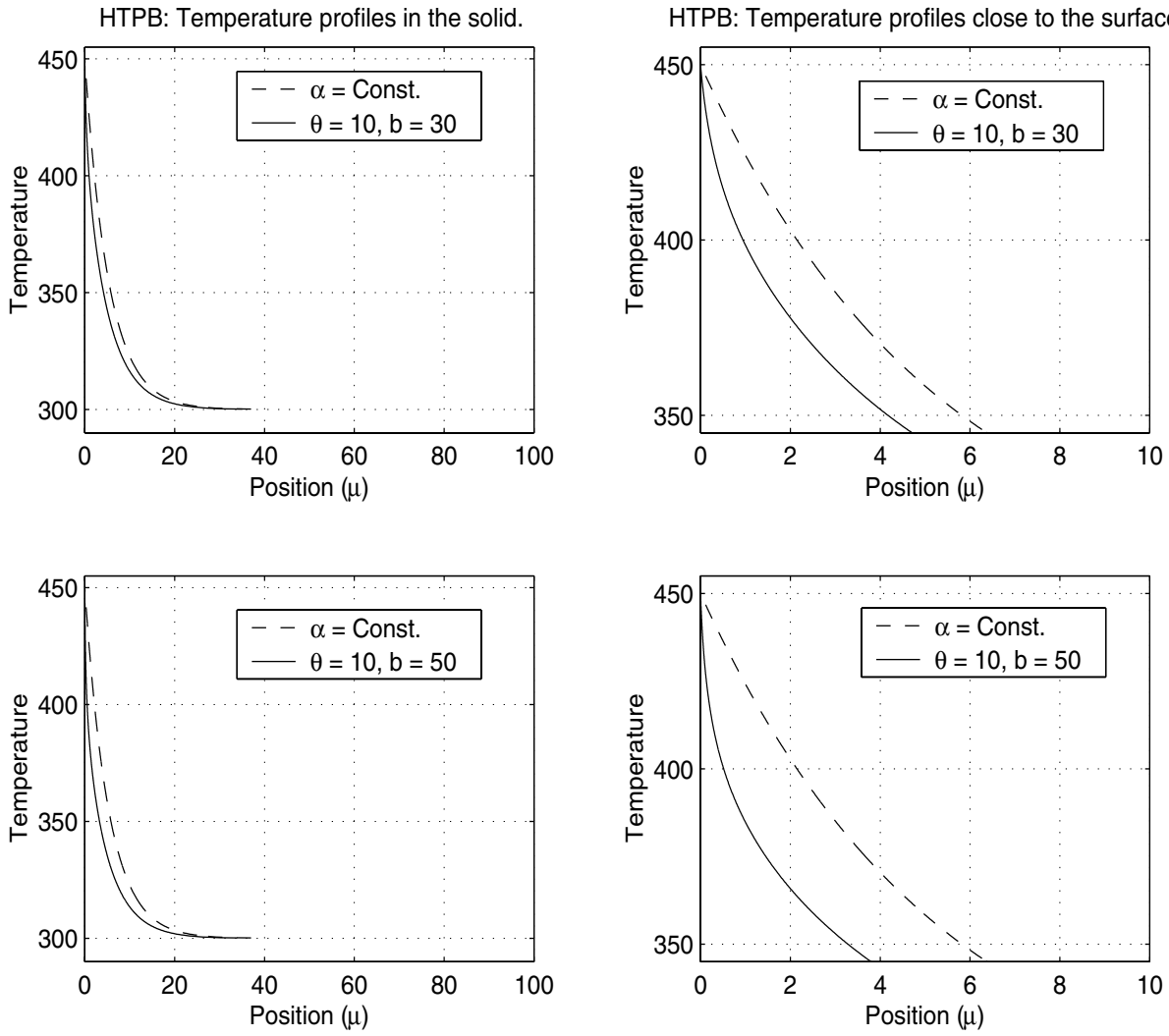

Figure 5: HTPB temperature profiles T(n) for two sets of curve fit parameters θ and b for $\alpha(T)$. Dotted line represents material with constant thermal expansion coefficient α_∞.

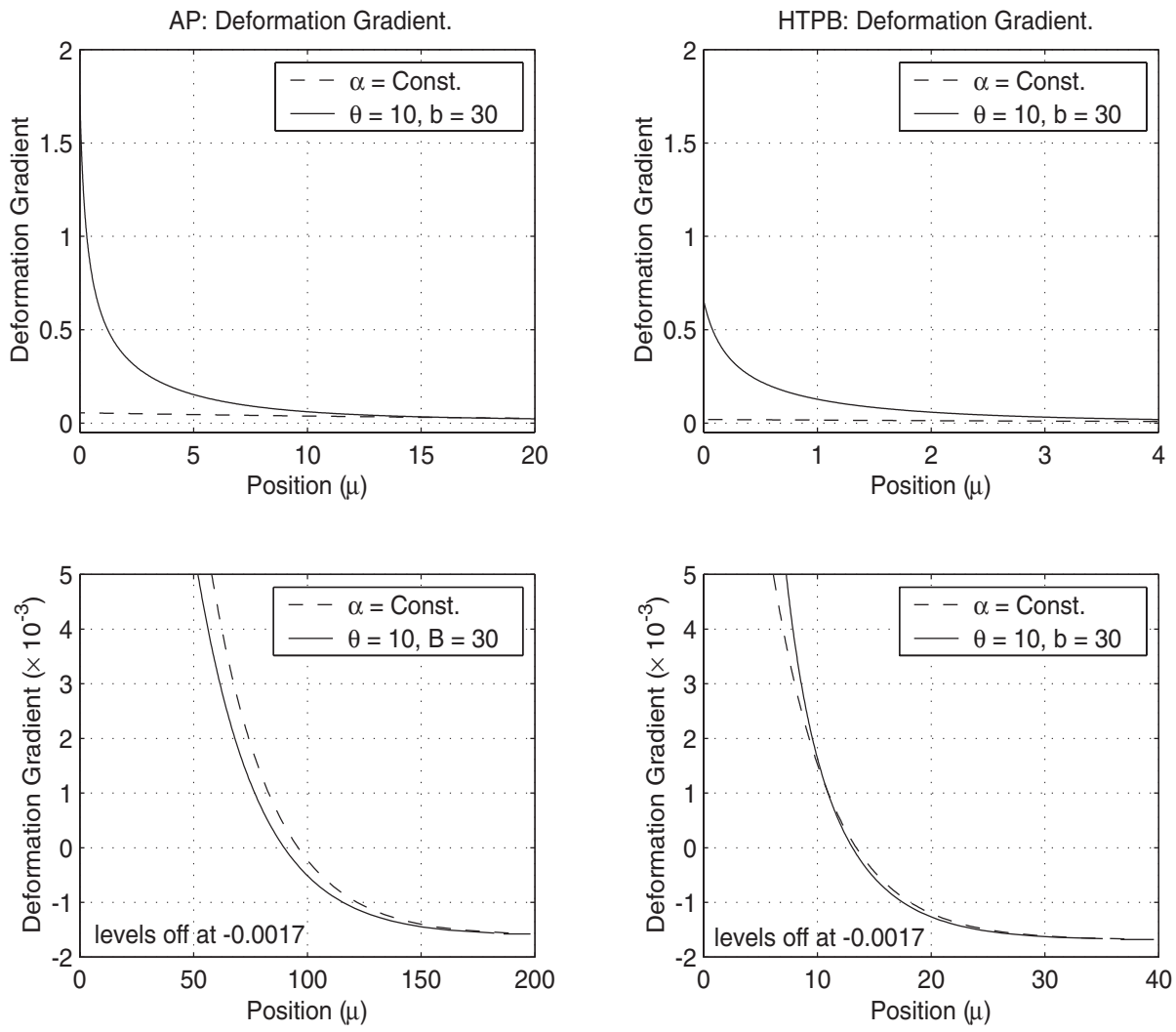

Figure 6: AP and HTPB deformation gradient profiles for $\theta = 10$ and $b = 30$ for $\alpha(T)$. Dotted line represents material with constant thermal expansion coefficient α_∞.

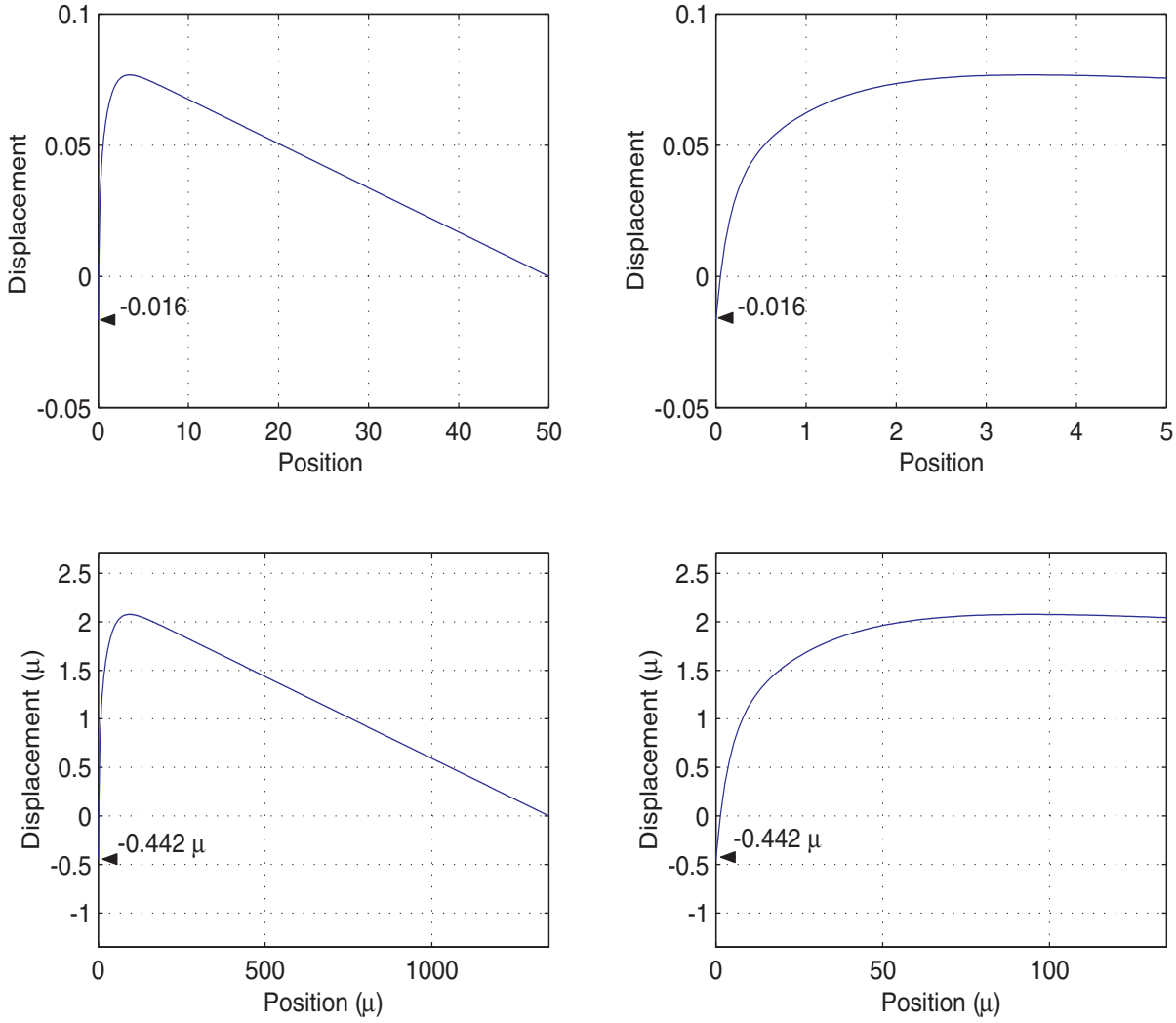

Figure 7: Instantaneous nondimensional (two upper plots) and dimensional displacement profiles in the layer of AP of thickness of 50 characteristic lengths (about 1.4mm), confined at the right hand side and with an interface on the left hand side.

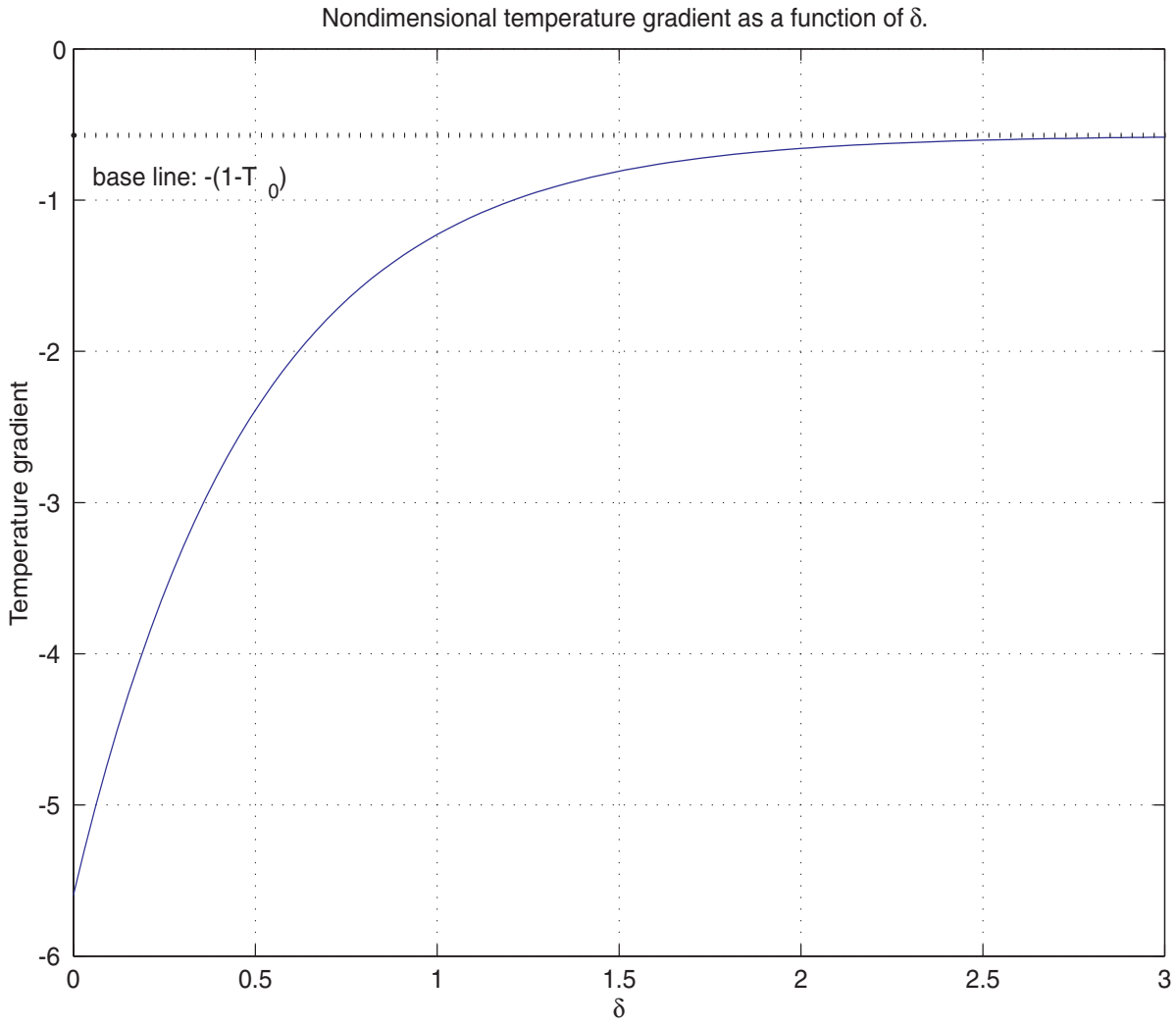

Figure 8: Heat flux at the surface as a function of δ.

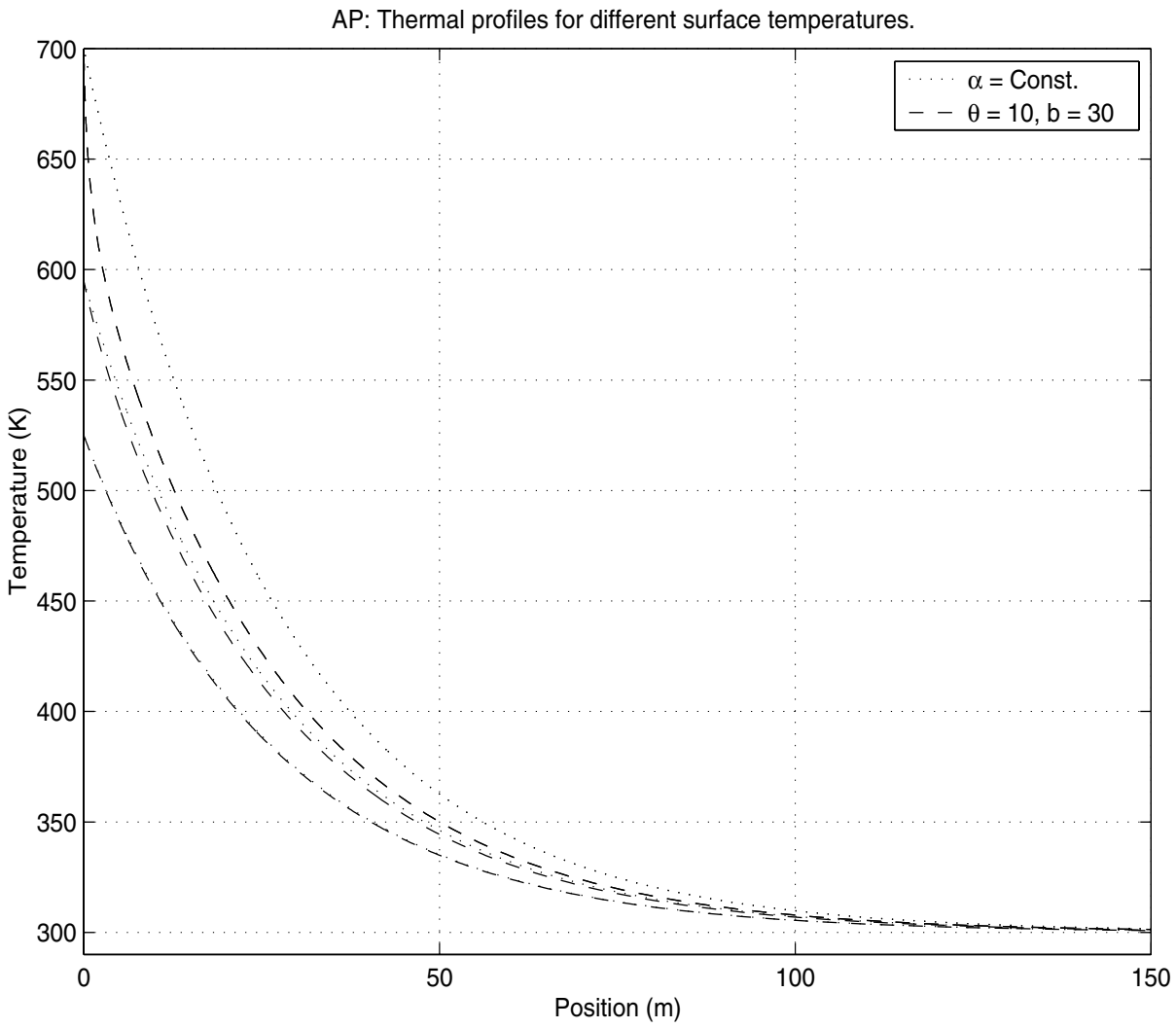

Figure 9: From bottom to top, δ is respectively 2.5, 1.5, 0 and θ is kept equal to 10. The bigger the value of δ, the less effect the is pronounced.

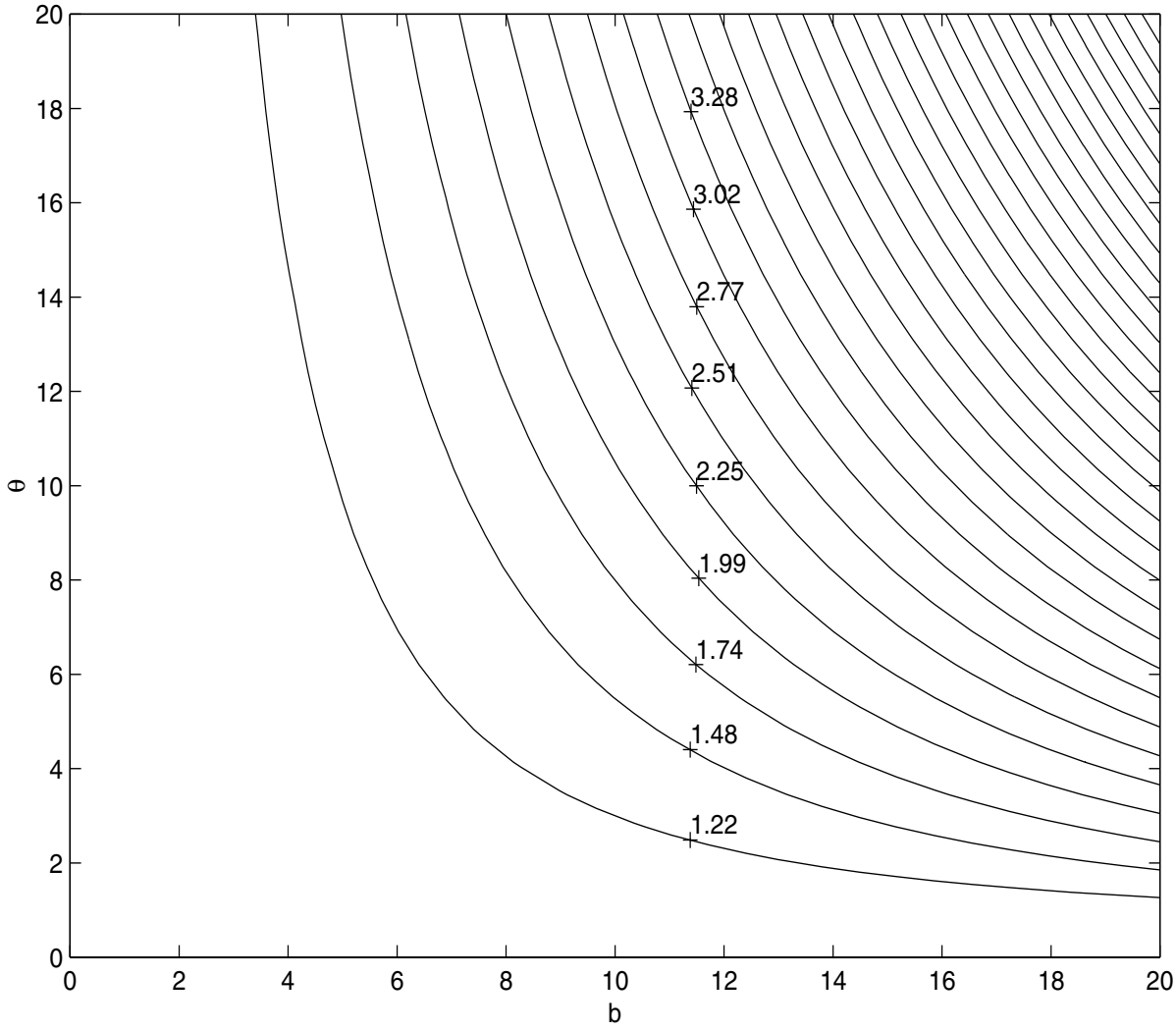

Figure 10: The contours of the ratio of the heat flux corresponding to the case with temperature dependent α to the base heat flux (b=0), for different values of b and θ .

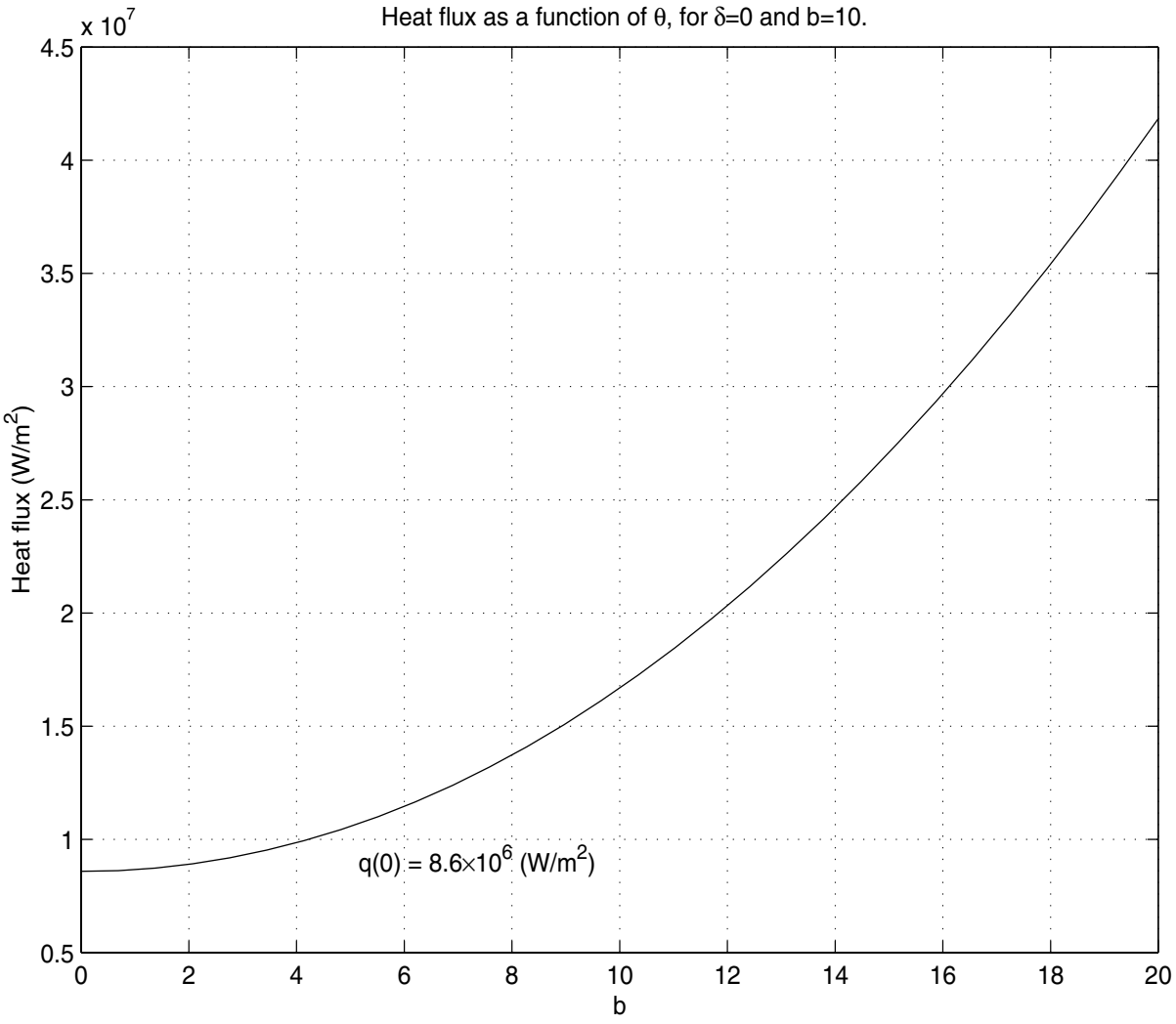

Figure 11: Heat flux to the solid for different values of b plotted for θ=10. Increasing values of b correspond to a larger endothermic effect in the near surface boundary layer.